Supporting Information

A Diprotonated Porphyrin as an Electron Mediator in Photoinduced Electron Transfer in Hydrogen-Bonded Supramolecular Assemblies

Wataru Suzuki,[†] Hiroaki Kotani,[†] Tomoya Ishizuka,[†] Masaki Kawano,[‡] Hayato Sakai,[⊥] Taku Hasobe,[⊥] Kei Ohkubo,[◊] Shunichi Fukuzumi,[§,¶] and Takahiko Kojima*[,†]

[†]*Department of Chemistry, Faculty of Pure and Applied Sciences, University of Tsukuba, 1-1-1 Tennoudai, Tsukuba, Ibaraki 305-8571, Japan*

[‡]*Department of Chemistry, School of Science, Tokyo Institute of technology, 2-12-1 Ookayama, Meguro-ku, Tokyo 152-8550, Japan*

[⊥]*Department of Chemistry, Faculty of Science and Technology, Keio University, Yokohama, 223-8522, Japan*

[◊]*Institute for Advanced Co-Creation Studies and Institute for Academic Initiatives, Osaka University, Suita, Osaka 565-0871, Japan*

[§]*Faculty of Science and Technology, Meijo University, Nagoya, Aichi 468-8502, Japan*

[¶]*Department of Chemistry and Nano Science, Ewha Womans University, Seoul 120-750, South Korea*

Contents

Experimental Section

Materials.

General. Solvents used for spectroscopic measurements (acetone, methanol, 2-methyltetrahydrofuran) were purchased from commercial sources and used without further purification. TFA and $Me_{10}Fc$ were purchased from commercial sources and used without further purification. $[Ru^{II}(\mu\text{-}Cl)(TPA)]_2(ClO_4)_2$,[1] and **$H_2$DPP**,[2,3] were synthesized according to the reported procedure. All ^{1}H NMR measurements were performed on JEOL JNM-ECS400, JNM-EX270, Bruker AVANCE400 and DPX400 spectrometers. UV-Vis absorption spectra were measured in spectroscopic-grade solvents on Shimadzu UV-2450 and UV-3600 spectrophotometers at room temperature. MALDI-TOF-MS spectra were measured on a Bruker UltrafleXtreme-TN and AB SCIEX TOF/TOF 5800 spectrometers using dithranol as a matrix. ESI-TOF-MS and CSI-TOF-MS spectra were measured on a JEOL JMS-T100CS spectrometer. The elemental analyses were made at Department of Chemistry, University of Tsukuba.

Synthesis.

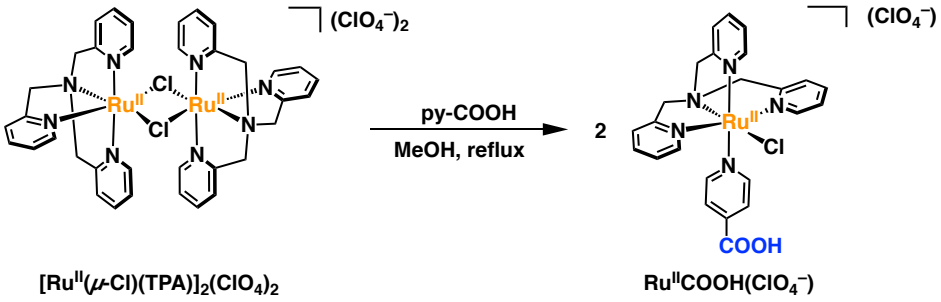

$[Ru^{II}(\mu\text{-}Cl)(TPA)]_2(ClO_4)_2$ $Ru^{II}COOH(ClO_4^-)$

$[Ru^{II}Cl(TPA)(pyCOOH)]^+(ClO_4^-)$ ($[Ru^{II}COOH](ClO_4^-)$). To a yellow suspension of $[Ru^{II}(\mu\text{-}Cl)(TPA)]_2(ClO_4)_2$ (102 mg, 97.4 μmol) in MeOH (15 ml), pyCOOH (32.2 mg, 262 μmol) was added and the resultant mixture was refluxed for 3 h under Ar. The mixture was concentrated to a small volume by a rotary evaporator. Diethyl ether was added to the solution to precipitate a mixture obtained as a red powder and a red crystalline solid. The red crystalline solid was manually collected to isolate $[Ru^{II}Cl(TPA)(pyCOOH)](ClO_4)$ (47.8 mg, 73.5 μmol) in 38% yield. ^{1}H NMR (acetone-d_6, 400 MHz): δ 4.70 (s, 2H, py_{axial}-CH_2-N), 4.82 (ABq, J_{AB} = 16 Hz, 2H, $py_{equatrial}$-CH_2-N), 5.08 (ABq, J_{AB} = 16 Hz, 2H, $py_{equatrial}$-CH_2-N), 7.18 (d, J = 7.8 Hz, 1H, H3 of py_{axial}), 7.30 (dd, J = 5.7 Hz, J = 7.8 Hz, 1H, H5 of py_{axial}), 7.47 (dd, J = 5.8 Hz, J = 7.7 Hz, 2H, H5 of $py_{equatrial}$), 7.60 (d, J = 7.7 Hz, 2H, H3 of $py_{equatrial}$), 7.61 (t, J = 7.8 Hz, 1H, H4 of py_{axial}), 7.69 (d, J = 6.9 Hz, 2H, H3 of py-COOH), 7.87 (t, J = 7.7 Hz, 2H, H4 of $py_{equatrial}$), 8.47 (d, J = 6.9 Hz, 2H, H2 of py-COOH), 9.17 (d, J = 5.8 Hz, 2H, H6 of $py_{equatrial}$), 9.88 (d, J = 5.7 Hz, 1H, H6 of py_{axial}). ESI-MS (MeOH): m/z = 455.03 (**M** – py-COOH – ClO_4^- + N_2), 550,03

((**M** – ClO_4^-) 572.04 (**M** – H^+ – ClO_4^- + Na^+). UV-Vis (acetone): λ_{max} (nm) = 436 ($\varepsilon = 1.5 \times 10^4$ M^{-1} cm^{-1}). Elemental analysis (%): Calcd for C24H23N5O2ClRu•ClO4•H2O: C 43.19, H 3.78, N 10.49; found: C 43.13, H 3.60, N 10.44.

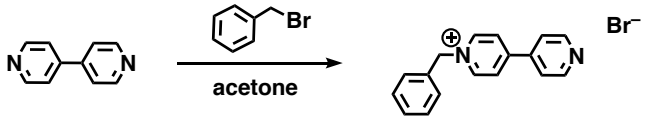

1-Benzyl-4,4'-bipyridinium bromide. To an acetone solution (5 mL) of 4,4'-bipyridyl (334 mg, 2.14 mmol), benzyl bromide (443 mg, 2.59 mmol) was added dropwise under Ar flow. The reaction mixture was heated at 60˚C for 23 h. After cooling the reaction mixture to room temperature, obtained solid was filtered to afford 1-benzyl-4,4'-bipyridinium bromide (643 mg, 1.96 mmol) in 96% yield. ^{1}H NMR (DMSO-d_6, 400 MHz): δ 5.92 (s, 2H, CH_2), 7.44-7.62 (m, 5H, Benzyl), 8.03 (d, J = 6.4 Hz, 2H, H3 for py), 8.64 (d, J = 6.8 Hz, 2H, H3 for Bn-py$^+$), 8.85 (d, J = 6.4 Hz, 2H, H2 for py), 9.38 (d, J = 6.8 Hz, 2H, H2 for Bn-py$^+$).

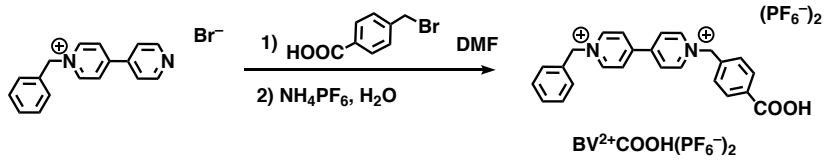

1-Benzyl-1'-(4-carboxyphenylmethyl)-4,4'-bipyridinium bishexafluorophosphate (BV^{2+}COOH(PF$_6^-$)$_2$). To a DMF solution (10 mL) of 1-benzyl-4,4'-bipyridinium bromide (141 mg, 0.431 mmol), 4-bromomethylbenzoic acid was added and the mixture was heated at 70 ˚C for 12 h. After cooling the reaction mixture to room temperature, obtained solid was filtered and washed with ether, then dried under vacuum to afford crude solid. The crude solid was dissolved in H_2O, then a saturated aqueous NH_4PF_6 solution was added to give colorless solid. The colorless solid was filtered to dried to obtain pure **BV^{2+}COOH**(PF$_6^-$)$_2$ (75.6 mg, 0.112 mmol) in 26% yield. ^{1}H NMR (acetone-d_6, 400 MHz): δ 6.18 (s, 2H, CH_2), 6.29 (s, 2H, CH_2), 7.51-7.70 (m, 5H, benzyl), 7.79 (d, J = 8.0 Hz, 2H, H2 of carboxyphenyl), 8.10 (d, J = 8.0 Hz, 2H, H3 of carboxyphenyl), 8.87 (d, J = 7.2 Hz, 2H, H3 for Bn-py$^+$), 8.88 (d, J = 7.2 Hz, 2H, H3 for carboxybenzyl-py$^+$), 9.58 (d, J = 7.2 Hz, 2H, H2 for Bn-py$^+$), 9.61 (d, J = 7.2 Hz, 2H, H2 for carboxybenzyl-py$^+$). ^{13}C NMR (acetone-d_6, 100 MHz): δ 168.8, 151.7, 151.5, 147.2, 146.9, 138.8, 134.2, 130.9, 130.5, 130.23, 130.20, 128.7, 128.6, 65.80, 65.19. Elemental analysis (%): Calcd for C25H22F12N2O2P2•0.25C3H6O: C 45.03, H 3.45, N 4.08; found: C 45.21, H 3.15, N 4.25.

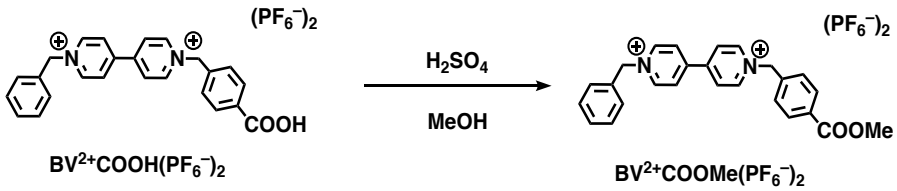

1-Benzyl-1'-(4-methoxycarboxyphenylmethyl)-4,4'-bipyridinium bishexafluorophosphate ($BV^{2+}COOMe(PF_6^-)_2$). A MeOH solution (5 mL) of $BV^{2+}COOH(PF_6^-)_2$ (39.7 mg, 0.0582 mmol) containing H_2SO_4 (1 drop) was refluxed for 3 days under Ar. The reaction mixture was concentrated, and small portion of H_2O was added. Then, a saturated aqueous NH_4PF_6 solution was added to give colorless solid. The colorless solid was filtered and dried to obtain pure $BV^{2+}COOMe(PF_6^-)_2$ (272.7 mg, 0.0403 mmol) in 71% yield. ^{1}H NMR (acetone-d_6, 400 MHz): δ 3.91 (s, 3H, COOMe), 6.20 (s, 2H, CH_2), 6.31 (s, 2H, CH_2), 7.51-7.69 (m, 5H, Benzyl), 7.79 (d, J = 8.6 Hz, 2H, H2 of methoxycarboxylphenyl), 8.10 (d, J = 8.6 Hz, 2H, H3 of methoxycarboxylphenyl), 8.87 (d, J = 6.8 Hz, 2H, H3 for Bn-py$^+$), 8.89 (d, J = 7.2 Hz, 2H, H3 for methoxycarboxybenzyl-py$^+$), 9.45 (d, J = 6.8 Hz, 2H, H2 for Bn-py$^+$), 9.59 (d, J = 7.2Hz, 2H, H2 for methoxycarboxybenzyl-py$^+$). ^{13}C NMR (acetone-d_6, 100 MHz): δ 166.5, 151.7, 151.4, 147.2, 146.9, 138.9, 134.2, 132.5, 131.2, 130.9, 130.5, 130.3, 130.2, 128.7, 128.6, 65.8, 65.1, 52.7. Elemental analysis (%): Calcd for C26H24F12N2O2P2: C 45.49, H 3.52, N 4.08; found: C 45.26, H 3.33, N 4.14.

Measurements.

X-ray Crystallography. Single crystals of **[Ru^{II}(Cl)(TPA)(pyCOOH)]**(ClO_4^-) were grown by vapor diffusion of diethyl ether into an acetone solution of **[Ru^{II}(Cl)(TPA)(pyCOOH)]**(ClO_4^-) at room temperature. Single crystals of **[H$_4$DPP^{2+}(Cl$^-$)(Ru^{II}COO$^-$)]**(ClO_4^-) were grown by vapor diffusion of 1,2-dichloroethane into an acetone solution of **H$_2$DPP** with 2 equivalents of **Ru^{II}COOH**(ClO_4^-) at 255 K. X-ray diffraction data of **[Ru^{II}(Cl)(TPA)(pyCOOH)]**(ClO_4^-) were obtained at 120 K on a Bruker APEXII Ultra diffractometer. Those of **[H$_4$DPP^{2+}(Cl$^-$)(Ru^{II}COO$^-$)]**(ClO_4^-) were obtained on a Rugaku Mercury CCD system at the Photon Factory-Advanced Ring for Pulse X-rays (PF-ARNW2A) of High Energy Accelerator Research Organization (KEK) at 183 K. The structures were solved by a direct method (SIR-97 or SIR-2014) and expanded with differential Fourier techniques. All non-hydrogen atoms were refined anisotropically and the refinements were carried out with full matrix least squares on *F*. All structure refinements were performed using the Yadokari-XG crystallographic software package.[4,5] In the structure refinements of **[H$_4$DPP^{2+}(Cl$^-$)(Ru^{II}COO$^-$)]**(ClO_4^-), contribution of the solvent molecules (6 molecules of 1,2-dichloroethane and 1 molecule of acetone) of crystallization were subtracted from the diffraction pattern by the "Squeeze" program.[6]

Supplementary crystallographic data of **[Ru^{II}(Cl)(TPA)(pyCOOH)]**(ClO_4^-) and **[H$_4$DPP^{2+}(Cl$^-$)(Ru^{II}COO$^-$)]**(ClO_4^-) are available from the Cambridge Crystallographic Data Centre as CCDC-1902314 and 1902315, respectively.

Spectroscopic Measurements. UV-Vis spectroscopic measurements were performed on a Shimadzu UV-2450 or UV-3600 spectrophotometer at 298 K. Fluorescence and phosphorescence spectra were measured on a HORIBA Fluorolog spectrofluorophotometer. Fluorescence spectra were measured in acetone at 298 K under air. ^{1}H NMR spectra were obtained on JEOL EX270, Bruker AVANCE400 and DPX400 spectrometers. For the NMR measurements for protonated species of H_2DPP, a certain amount of acids (**Ru^{II}COOH**(ClO_4^-), TFA, or **BV^{2+}COOH(PF$_6^-$)$_2$**) were added to a solution of **H$_2$DPP** in acetone-d_6 with 1,4-dioxane as an internal standard.

Electrochemical Measurements. Cyclic voltammetry (CV) and differential pulse voltammetry (DPV) measurements were carried out in acetone containing 0.1 M $TBAPF_6$ or $TBAClO_4$ as an electrolyte at 298 K under Ar. All measurements were made using a BAS ALS-710D electrochemical analyzer with a grassy carbon working electrode or platinum disk working electrode, a platinum wire as a counter electrode, and $Ag/AgNO_3$ as a reference electrode. All redox potentials were determined relative to that of Fc/Fc^+ as 0 V.

Femtosecond Laser Flash Photolysis Measurements. The source for the pump and probe pulses were derived from the fundamental output of Integra-C (780 nm, 2 mJ/pulse and fwhm = 130 fs) at a repetition rate of 1 kHz. A total of 75% of the fundamental output of the laser was introduced into TOPAS, which has optical frequency mixers resulting in tunable range from 285 to 1660 nm, while the rest of the output was used for white light generation. Prior to generating the probe continuum, a variable neutral density filter was inserted in the path to generate stable continuum, and then the laser pulse was fed to a delay line that provides an experimental time window of 3.2 ns with a maximum step resolution of 7 fs. In our experiments, a wavelength at 500 nm of TOPAS output, which is the fourth harmonic of signal or idler pulses, was chosen as the pump beam. As this TOPAS output consists of not only desirable wavelength but also unnecessary wavelengths, the latter was deviated using a wedge prism with wedge angle of 18º. The desirable beam was irradiated at the sample dell with a spot size of 1 mm diameter where it was merged with the white probe pulse in a close angle (<10º). The probe beam after passing through the 2 mm sample cell was focused on a fiber optic cable that was connected to a CCD spectrograph for recording the time-resolved spectra (500 – 1200 nm). Typically, 2500 excitation pulses were averaged for 5 s to obtain the transient spectrum at a set delay time. Kinetic traces at appropriate wavelengths were assembled from the time-resolved spectral data.

Picosecond Laser Flash Photolysis Measurements. Picosecond time-resolved transient absorption measurements were conducted using the device manufactured by Unisoku Co., Ltd. Measurement method used in this instrument was randomly-interleaved-pulse-train (RIPT) method.[7] The measurements were performed according to the following procedure: A deaerated solution in 2 mm sample cell was excited by a Nd:YAG micro laser (1 kHz, 200 ps, 532 nm). The probe source is a supercontinuum radiation source (2W 20 MHz, 50 – 100 ps, 410 – 2000 nm). Photochemical reactions were monitored in the range from 500 to 700 nm.

Nanosecond Laser Flash Photolysis Measurements. Nanosecond time-resolved transient absorption measurements were performed using a laser system provided by UNISOKU Co., Ltd. The measurements were performed according to the following procedure: A deaerated solution was excited by a Panther optical parametric oscillator pumped by a Nd:YAG laser (Continuum, SLII-10, 4-6 ns fwhm) at λ = 532 nm. Photochemical reactions were monitored (500 –700 nm) by continuous exposure to a xenon lamp (150 W) as a probe light and a photomultiplier tube (Hamamatsu 2949) as a detector.

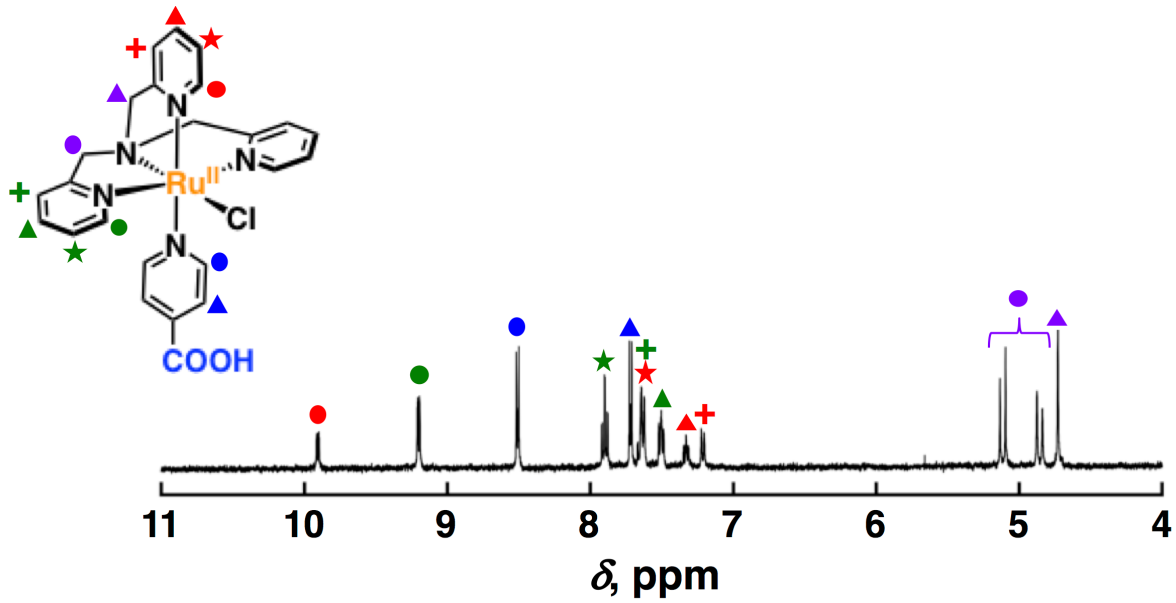

Figure S1. ^{1}H NMR spectrum of **Ru^{II}COOH**(ClO_4^-) in acetone-d_6.

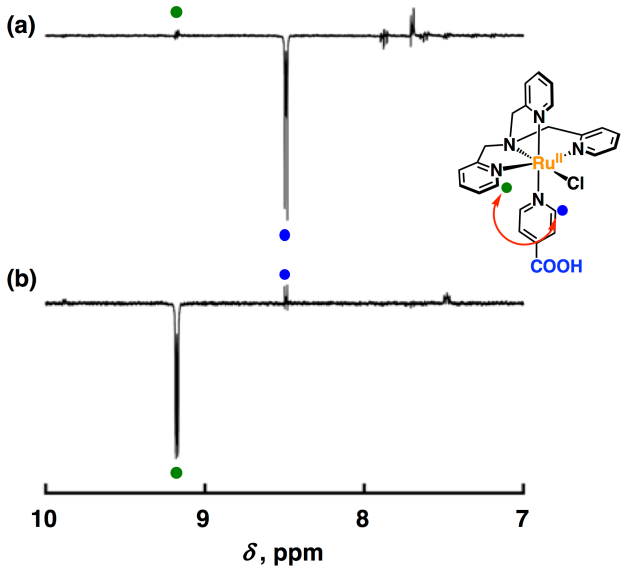

Figure S2. NOE measurements of **Ru^{II}COOH**(ClO_4^-) in acetone-d_6. (a) Differential ^{1}H NMR spectrum of **Ru^{II}COOH**(ClO_4^-) with and without irradiation of the signal due to the protons of the 2-positions of pyCOOH (blue circle). (b) Differential ^{1}H NMR spectrum of **Ru^{II}COOH**(ClO_4^-) with and without irradiation of the signals due to the protons of the 6-positions of the equatorial pyridine rings of TPA (green circle).

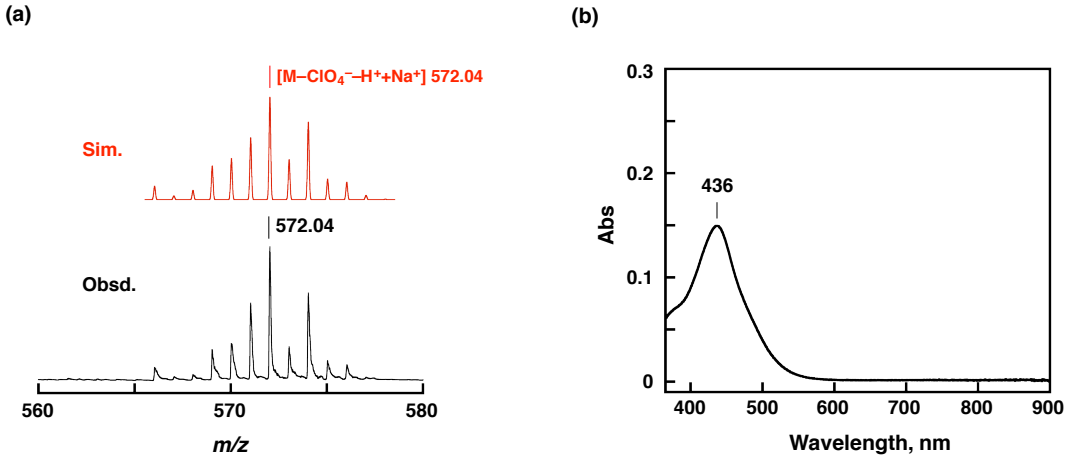

Figure S3. (a) ESI-TOF-MS of **Ru^{II}COOH**(ClO_4^-) in methanol. (b) UV-Vis absorption spectrum of **Ru^{II}COOH**(ClO_4^-) in acetone.

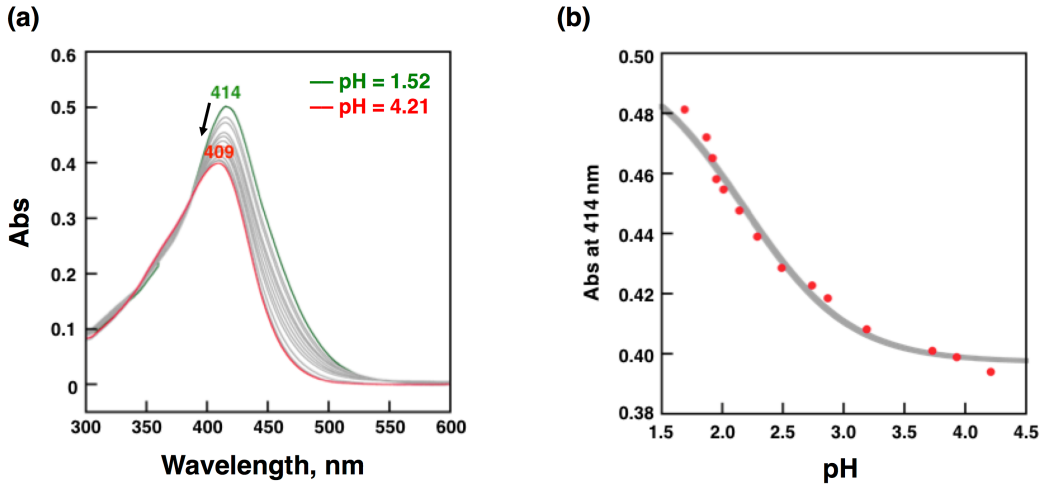

Figure S4. (a) pH-dependent absorption spectral change of **Ru^{II}COOH**(ClO_4^-) (0.040 mM) in Briton-Robinson buffer (0.1 M) upon addition of 8 M $NaOH_{aq}$ at 298 K; green: pH = 1.52, red: pH = 4.21. (b) Plot of absorbance at 414 nm vs pH.

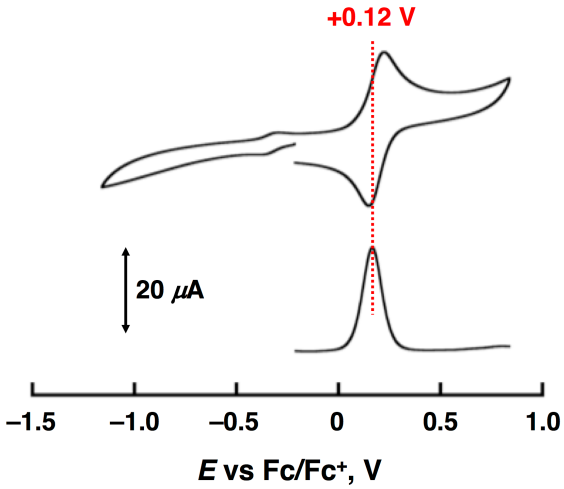

Figure S5. CV (top) and DPV (bottom) of $\mathbf{Ru^{II}COOH}(ClO_4^-)$ (1.0 mM) in acetone containing 0.1 M $TBAClO_4$ as an electrolyte at 298 K under Ar.

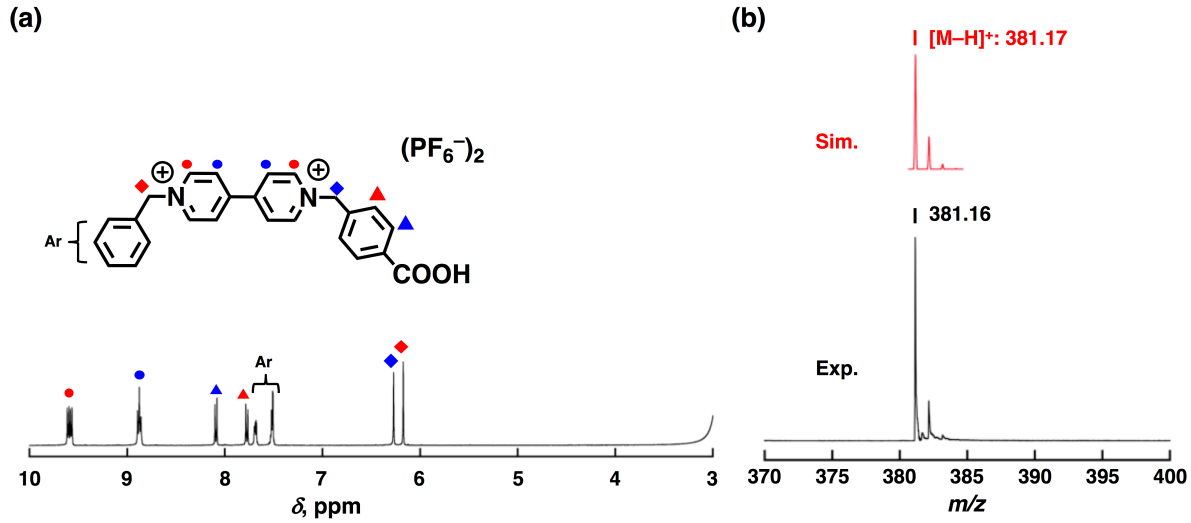

Figure S6. (a) ^{1}H NMR spectrum of $\mathbf{BV^{2+}COOH}(PF_6^-)_2$ in acetone-d_6. (b) ESI-TOF-MS spectrum of $\mathbf{BV^{2+}COOH}(PF_6^-)_2$ in MeOH (black) with its computer simulation (red).

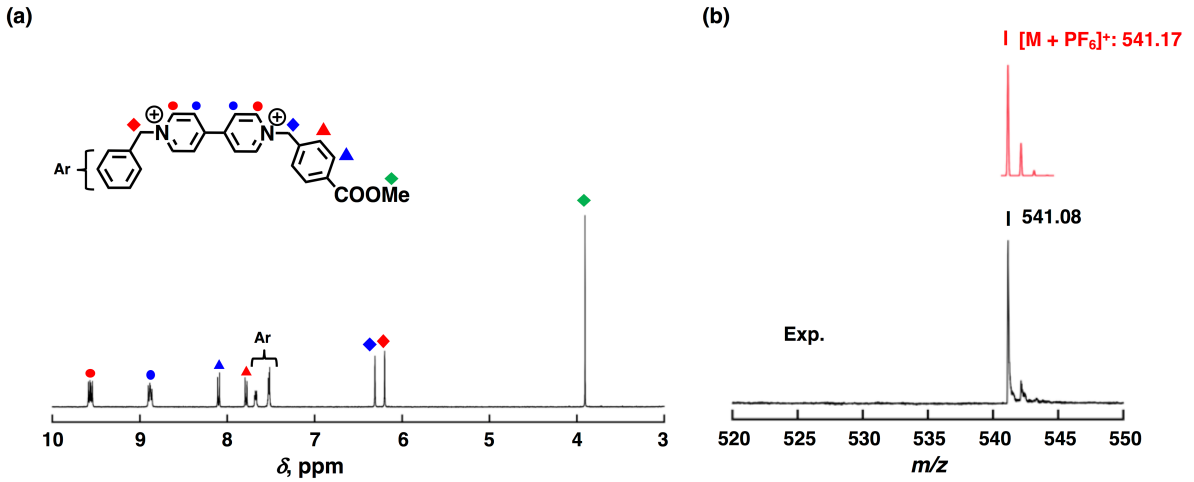

Figure S7. (a) ^{1}H NMR spectrum of **BV^{2+}COOMe**(PF_6^-)$_2$ in acetone-d_6. (b) ESI-TOF-MS spectrum of **BV^{2+}COOMe**(PF_6^-)$_2$ in MeOH (black) with its computer simulation (red).

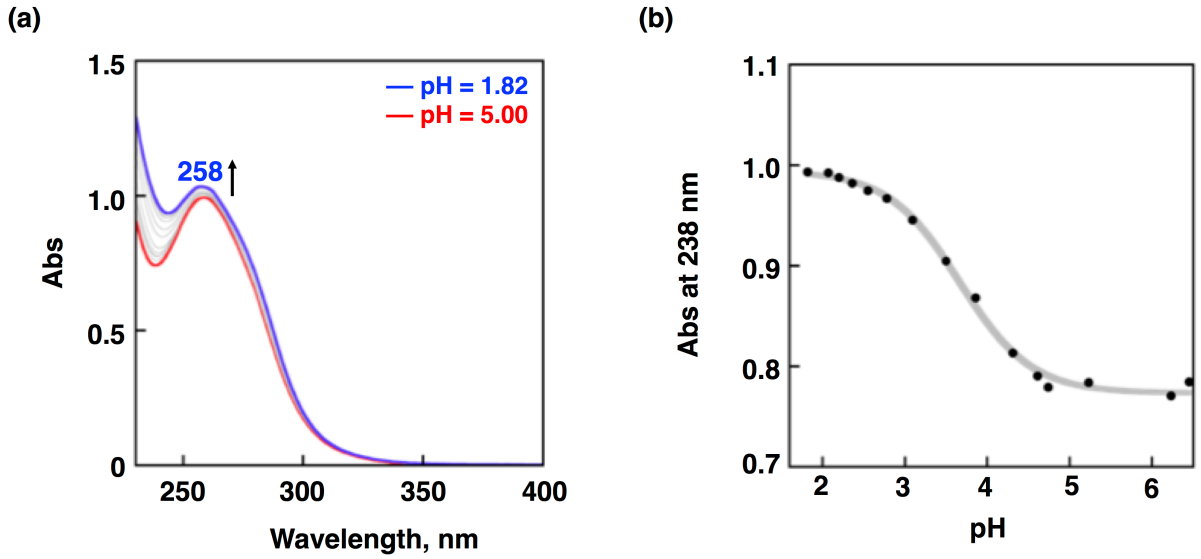

Figure S8. (a) pH-dependent absorption spectral change of **BV**$^{2+}$**COOH**(PF_6^-)$_2$ (0.40 mM) in Briton-Robinson buffer (0.1 M) upon addition of 4 M $HClO_4$aq at 298 K; red: pH = 5.00, blue: pH = 1.82. (b) Plot of absorbance at 238 nm vs pH.

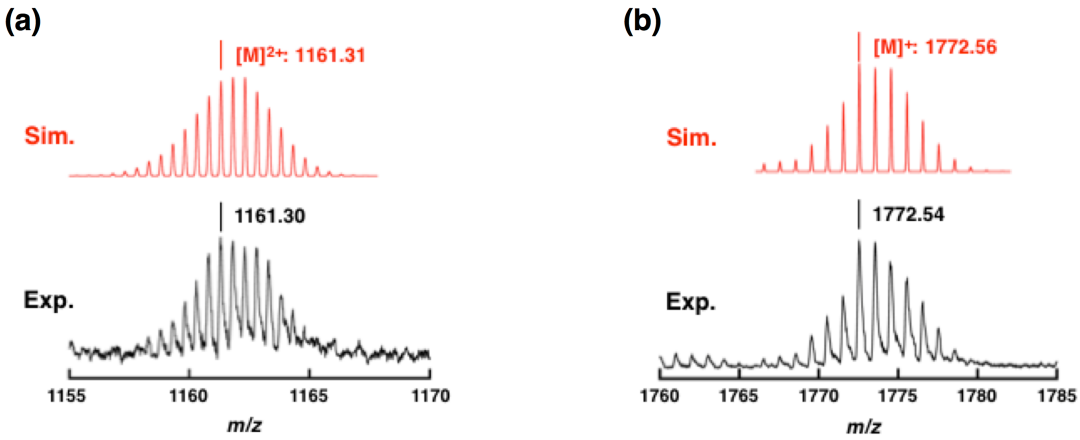

Figure S9. CSI-TOF-MS of (a) $[\mathbf{H_4DPP^{2+}}(\mathbf{Ru^{II}COO^-})_2]^{2+}$ and (b) $[\mathbf{H_3DPP^+}(\mathbf{Ru^{II}COO^-})]^+$ in acetone/methanol (97/3 (v/v)) at –80˚C. Sim. (top), Exp. (bottom).

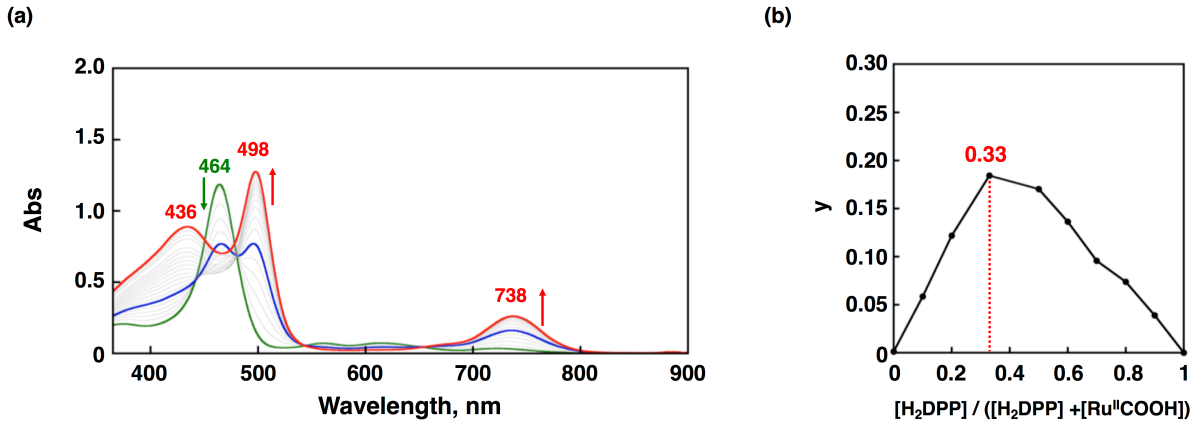

Figure S10. (a) UV-Vis absorption spectral change of **H_2DPP** (8.8 μM) upon adding **Ru^{II}COOH** in acetone at 298 K; green; **H_2DPP**, blue: **H_2DPP** + 1 eq of **Ru^{II}COOH**, purple: **H_2DPP** + 2 eq of **Ru^{II}COOH**, red: **H_2DPP** + 4 eq of **Ru^{II}COOH**. (b) A Job's continuous plot for the association of **H_2DPP** with **Ru^{II}COOH** in acetone at 298 K. y = Abs. – (ε_1 [**H_2DPP**] + ε_2 [**Ru^{II}COOH**]); ε_1: a molecular extinction coefficient of **H_2DPP** at 738 nm, ε_2: a molecular extinction coefficient of **Ru^{II}COOH** at 738 nm. [**H_2DPP**] + [**Ru^{II}COOH**] = 9.0×10^{-5} M.

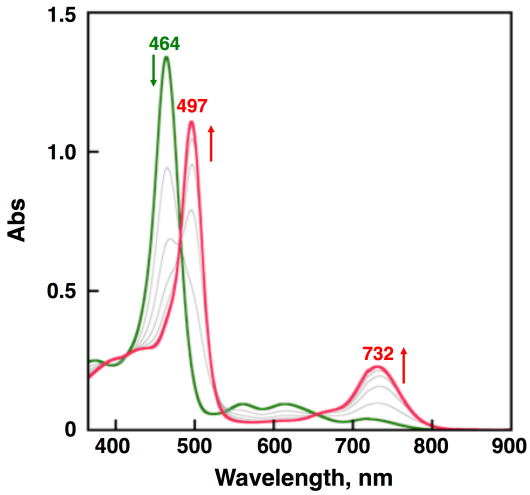

Figure S11. UV-Vis absorption spectral change of **H_2DPP** upon addition of **BV^{2+}COOH**(PF_6^-)$_2$ in acetone at room temperature. Green: **H_2DPP**, Red: **H_2DPP** with 6 equiv of **BV^{2+}COOH**(PF_6^-)$_2$.

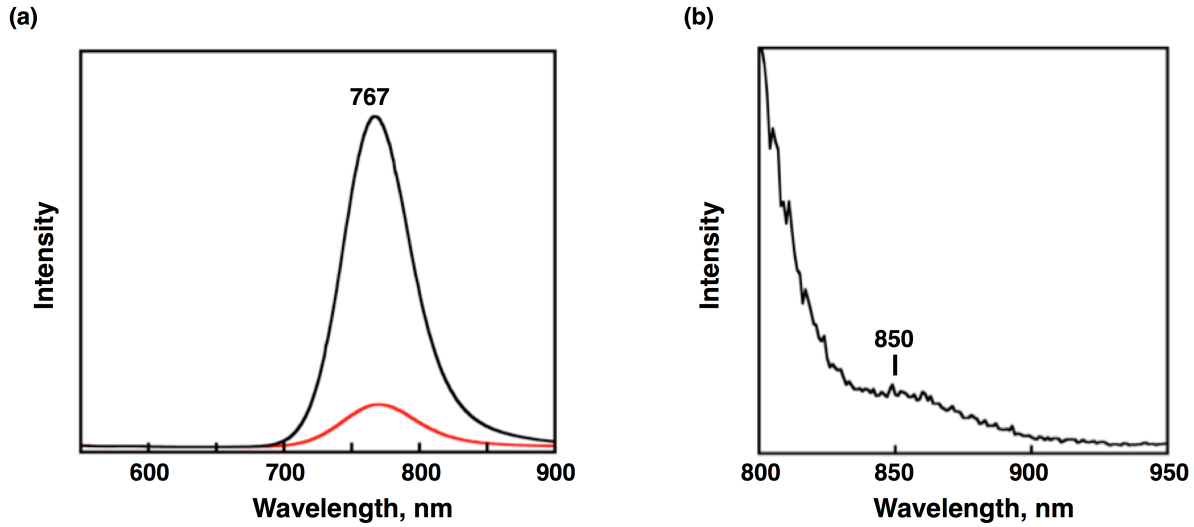

Figure S12. (a) Fluorescence spectra of $\mathbf{H_4DPP^{2+}(Ru^{II}COO^-)_2}$ (red) in acetone obtained by photoirradiation (λ_{ex} = 500 nm) at room temperature; black: $\mathbf{H_4DPP^{2+}(CF_3COO^-)_2}$ as references: [$\mathbf{H_2DPP}$] = 7.9 μM, [$\mathbf{Ru^{II}COOH}(ClO_4^-)$] = 16 μM. (b) Phosphorescence spectrum of $\mathbf{H_4DPP^{2+}(CF_3COO^-)_2}$ in a 2-MeTHF glass obtained by photoirradiation (λ_{ex} = 500 nm) at 77 K; [$\mathbf{H_2DPP}$] = 16 μM, [CF_3COOH] = 0.15 mM.

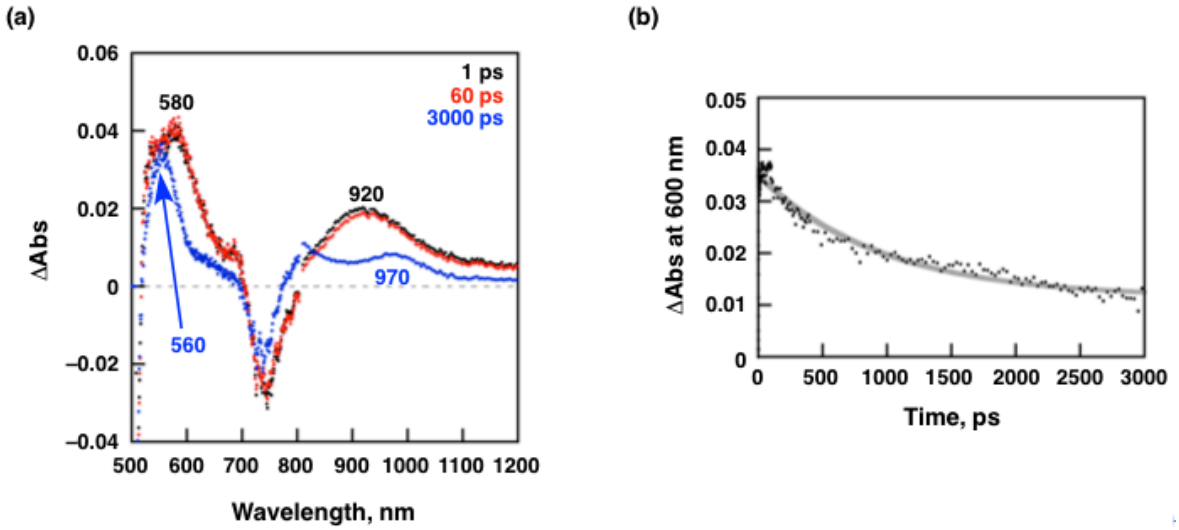

Figure S13. (a) Time-resolved transient absorption spectra (λ_{ex} = 500 nm) of $\mathbf{H_4DPP^{2+}(CF_3COO^-)_2}$ (0.050 mM) in deaerated acetone at 1 ps (black), 60 ps (red), and 3000 ps (blue) after femtosecond laser excitation at 500nm. (b) Decay time profile of $^1[\mathbf{H_4DPP^{2+}}]^*$ monitored at 600 nm with single exponential decay curve fitting: $[\mathbf{H_2DPP}]_0 = 5.0 \times 10^{-5}$ M, [TFA] = 1.0×10^{-4} M.

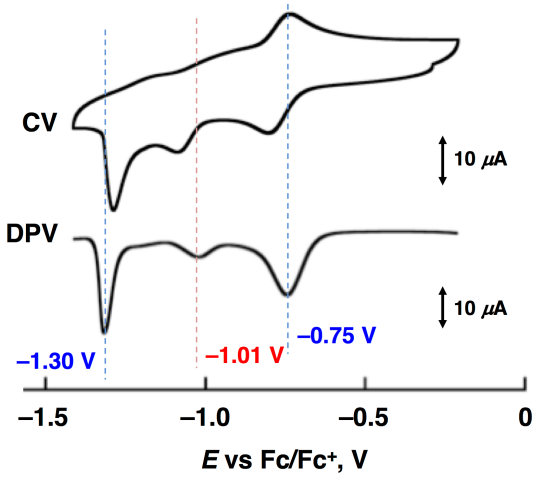

Figure S14. CV and DPV of **H_2DPP** (0.29 mM) in the presence of 2 equivalents of **BV^{2+}COOH**(PF_6^-)$_2$ in deaerated acetone containing 0.1 M TBAPF_6 at 298 K. Scan rate = 100 mV /s.

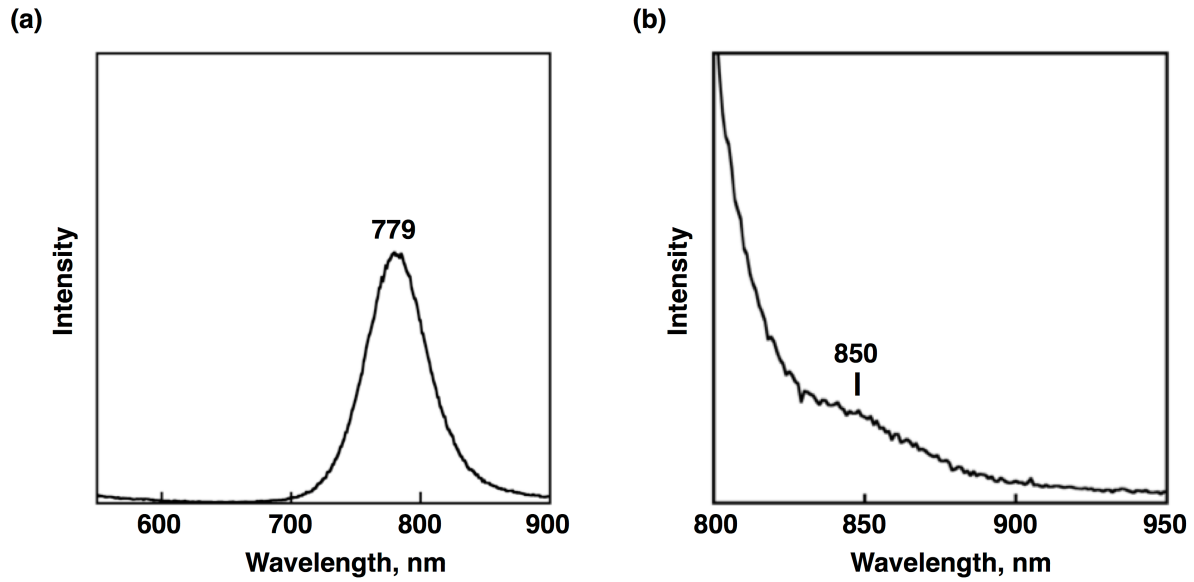

Figure S15. (a) Fluorescence spectrum of $\mathbf{H_4DPP^{2+}(BV^{2+}COO^{-})_2}$ in acetone obtained by photoirradiation (λ_{ex} = 500 nm) at room temperature. (b) Phosphorescence spectrum of $\mathbf{H_4DPP^{2+}(BV^{2+}COO^{-})_2}$ in a 2-MeTHF glass obtained by photoirradiation (λ_{ex} = 500 nm) at 77 K.

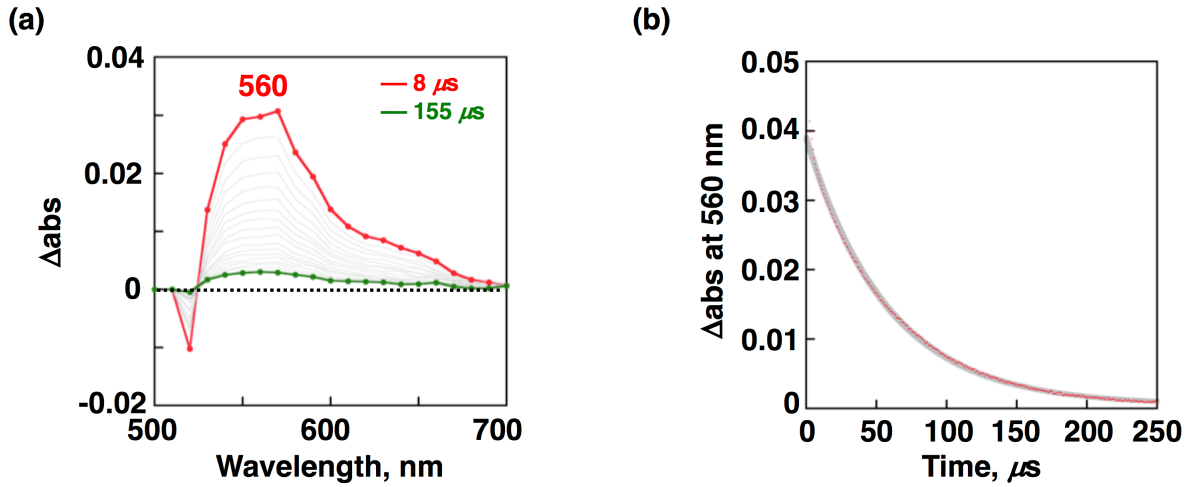

Figure S16. (a) Time-resolved nanosecond transient absorption spectra (λ_{ex} =532 nm) of $\mathbf{H_4DPP^{2+}(BV^{2+}COO^{-})_2}$ (0.050 mM) in deaerated acetone at 8 μs (red), and 155 μs (green) after laser excitation at 532 nm. (b) Single exponential decay of $^3[\mathbf{H_4DPP^{2+}}]^*$ monitored at 560 nm: $[\mathbf{H_2DPP}] = 5.0 \times 10^{-5}$ M, $[\mathbf{BV^{2+}COOH}] = 2.0 \times 10^{-4}$ M.

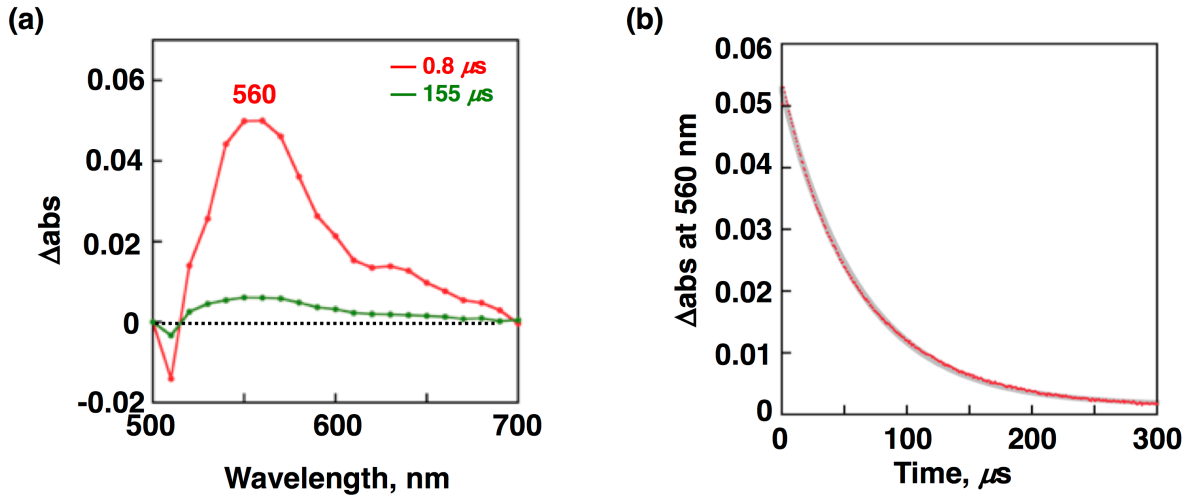

Figure S17. (a) Transient absorption spectra (λ_{ex} =532 nm) of $\mathbf{H_4DPP^{2+}(CF_3COO^-)_2}$ (0.050 mM) in deaerated acetone at 0.8 μs (red), and 155 μs (green) after nanosecond laser excitation at 532 nm. (b) Decay time profile of $^3[\mathbf{H_4DPP^{2+}}]^*$ monitored at 560 nm with single exponential decay curve fitting: $[\mathbf{H_2DPP}] = 5.0 \times 10^{-5}$ M, $[CF_3COOH] = 2.0 \times 10^{-4}$ M.

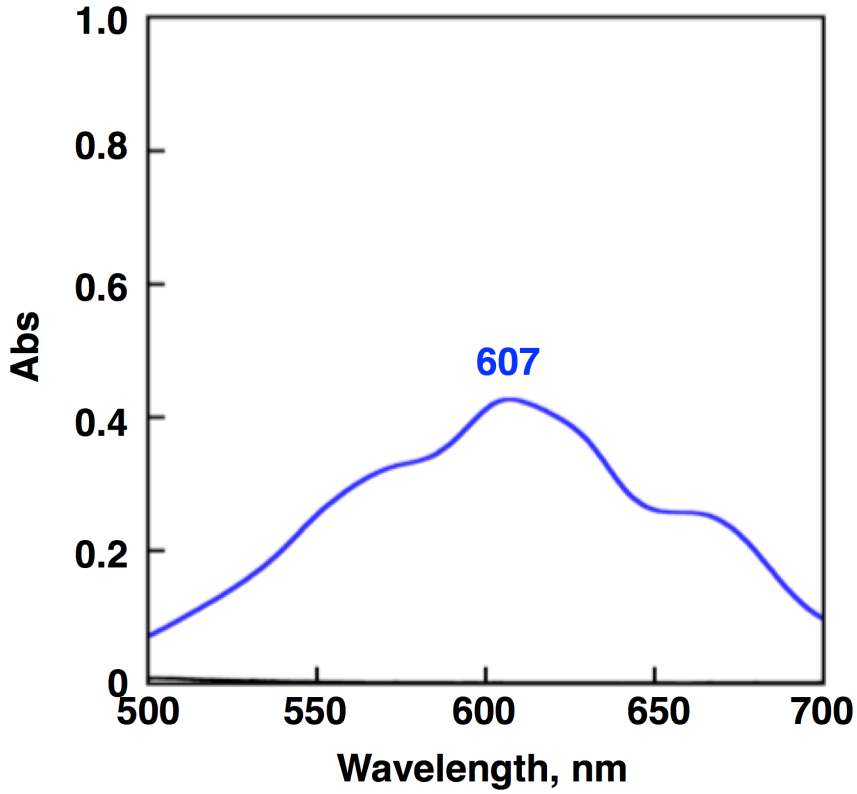

Figure S18. UV-Vis absorption spectrum of **$BV^{2+}COOH$** with 1 equivalent of $Na_2S_2O_4$aq in deaerated acetone.

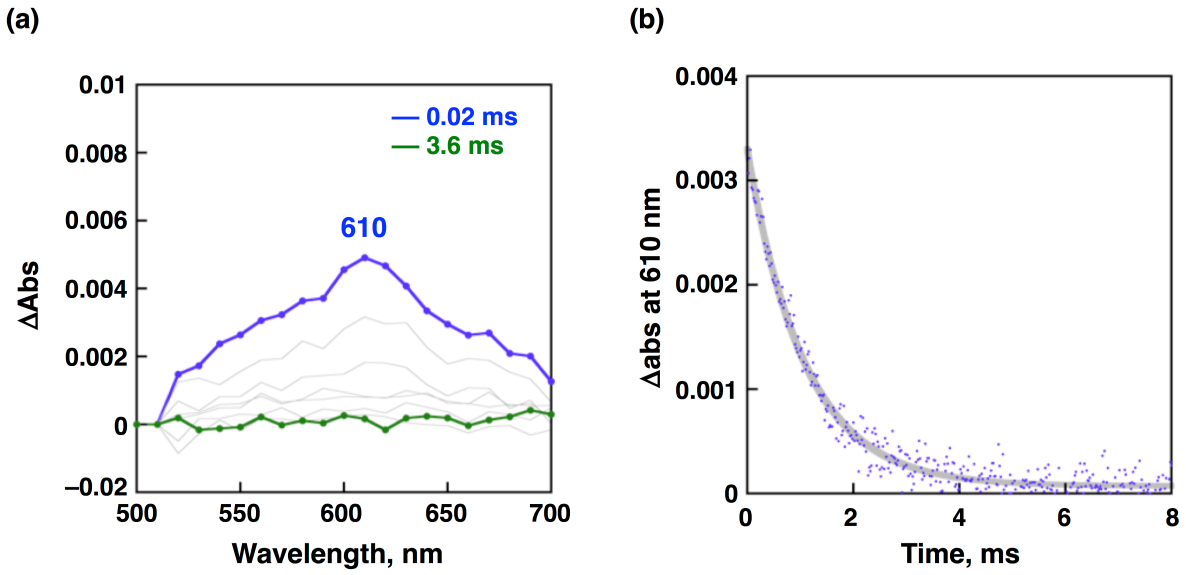

Figure S19. (a) Time-resolved transient absorption spectra (λ_{ex} = 532 nm) of $\mathbf{H_4DPP^{2+}(BV^{2+}COO^-)_2}$ (0.050 mM) with $Me_{10}Fc$ (0.60 mM) in deaerated acetone at 0.02 ms (blue), and 3.6 ms (green) after nanosecond laser excitation at 532 nm. (b) Decay time profile of $^3[\mathbf{H_4DPP^{2+}}]^*$ monitored at 610 nm with single exponential decay curve fitting: $[\mathbf{H_2DPP}]_0$ = 5.0×10^{-5} M, $[\mathbf{BV^{2+}COOH}] = 2.0 \times 10^{-4}$ M.

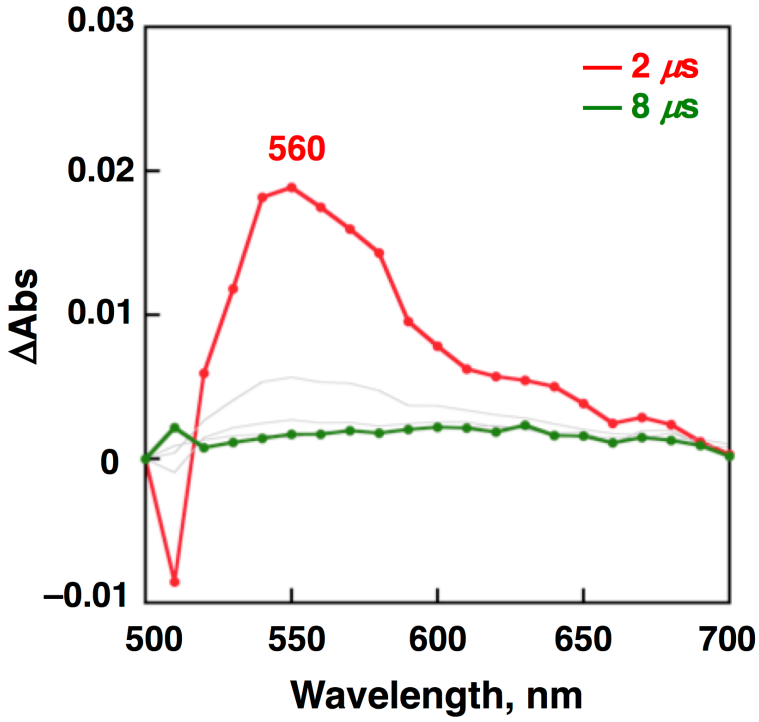

Figure S20. Transient absorption spectra (λ_{ex} = 532 nm) of $\mathbf{H_4DPP^{2+}(CF_3COO^-)_2}$ (0.050 mM) with $Me_{10}Fc$ (0.60 mM) and $\mathbf{BV^{2+}COOMe}$ (0.20 mM) in deaerated acetone at 2 μs (red), and 8 μs (green) after nanosecond laser excitation at 532 nm. $[\mathbf{H_2DPP}]_0 = 5.0 \times 10^{-5}$ M. $[CF_3COOH] = 2.0 \times 10^{-4}$ M.

Table S1. Crystallographic data for **[Ru^{II}(Cl)(TPA)(pyCOOH)]**(ClO_4^-) and **[H_4DPP^{2+}(Cl^-)($Ru^{II}COO^-$)]**(ClO_4^-).

compound	**[Ru^{II}(Cl)(TPA)(pyCOOH)]**(ClO_4^-)	**[H_4DPP^{2+}(Cl^-)($Ru^{II}COO^-$)]**(ClO_4^-)
crystal system	monoclinic	monoclinic
space group	$P2_1/c$	$P2_1/c$
T, K	120	183
formula	$C_{24}H_{23}ClN_5O_2Ru•ClO_4$	$C_{92}H_{64}N_4$• $C_{24}H_{22}ClN_5O_2Ru•Cl•ClO_4$
FW	649.45	1909.44
a, Å	9.680(4)	17.8208(2)
b, Å	15.744(6)	28.4808(4)
c, Å	16.612(6)	27.2786(4)
α, deg	90	90
β, deg	98.865(6)	99.8014(15)
γ, deg	90	90
V, Å^3	2501.5(16)	13643.2(3)
Z	4	4
λ, Å	0.71073 (MoKα)	0.6889 (synchrotron)
D_c, g cm^{-3}	1.724	0.930
reflns measured	8452	177037
reflns unique	2924	33185
R_1 ($I >$ 2σ(I))	0.0585	0.0771
wR_2 (all)	0.1381	0.2340
GOF	1.083	1.027

References

1. Kojima, T.; Amano, T. Ishii, Y.; Ohba, M.; Okaue, Y.; Matsuda, Y. *Inorg. Chem.* **1998**, *37*, 4076-4085.
2. Medforth, C. J.; Senge, M. O.; Smith, K. M.; Sparks, L. D. Shelnutt, J. A. *J. Am. Chem. Soc.* **1992**, *114*, 9859-9869.
3. Liu, C.-J.; Yu, W.-Y.; Peng, S.-M.; Mak, C. W.; Che, C.-M. *J. Chem. Soc., Dalton Trans.* **1998**, *11*, 1805–1812.
4. Wakita, K. Yadokari-XG, Software for Crystal Structure Analyses **2001**.
5. Kabuto, C.; Akine, S.; Nemoto, T.; Kwon, E. *J. Cryst. Soc. Jpn.* **2009**, *51*, 218-224.
6. Spek, A. L. D. *Acta Crystallogr. Sect. C: Struct. Chem.* **2015**, *71*, 9-18.
7. Nakagawa, T.; Okamoto, K.; Hanada, H.; Katoh, R. *Opt. Lett.* **2016**, *41*, 1498-1501.